

Proceedings of International Conference
Applications of Structural Fire Engineering
Prague, 19-20 February 2009

Session 7

Timber Structures

549

TESTS AND MODELLING OF WOOD IN SHEAR AT ELEVATED TEMPERATURES

Maxime Audebert ^{a,b}, Abdelhamid Bouchaïr ^a, Dhionis Dhima ^b

^a LaMI, Civil Engineering, Blaise Pascal University, Clermont-Ferrand, France

^b CSTB, Centre Scientifique et Technique du Bâtiment, Marne-la-Vallée, France

INTRODUCTION

Fire safety remains a major subject of interest for the development of the use of wood in building structures. Wood is a combustible material but several research works showed that the thermo-mechanical behaviour of timber structures exhibit an interesting behaviour in fire situations [1-3]. In fact, the charring rate of timber elements is generally well known. Consequently, the decrease of the fire resistance of structures can be predicted if the evolution of the wood properties, with temperature, is known.

Besides, the structural joint are characterised by various complex geometrical and material configurations due mainly to the orthotropic character of wood. However, a limited number of studies are available concerning the timber joints. Thus, a modelling approach combined with experimental tests is chosen to evaluate the behaviour of dowelled steel-to-timber joints with the aim of developing simple design rules [8]. The modelling needs many data about the material characteristics of wood mainly in shear. In EN 1995-1-2 [4], the reduction factors for strength (compression, tension and shear) are given for softwood, in the direction parallel to grain. For compression perpendicular to grain or shear parallel to grain, the same reduction of strength may be applied as for compression parallel to grain. In this study, an experimental study is used to validate this hypothesis. Thus to provide the material characteristics to be used in the numerical model of the timber-to-timber and the steel-to-timber dowelled connections, tests are performed to determine the shear reduction factors of glulam under high temperatures.

This paper presents the results of shear tests of glulam samples under high temperatures. At first, these original tested specimens are described and their geometry justified. Then, the testing program and the results are discussed and compared to the values given by EC5. The final aim of the study is to analyse the thermo-mechanical properties of wood in shear to be included in a more extensive study on the modelling of the thermo-mechanical behaviour of timber connections.

1 SHEAR TEST SPECIMENS AND TEST ARRANGEMENT

The experimental tests carried out at CSTB (Marne-la-Vallée, France) concern 9 specimens taken from glulam members with a moisture content of 8%. The average density measured varied between 433 and 462 kg/m³ which correspond to wood in class GL24h [5]. The specimens are characterised by an original geometry (Fig. 1). The cylindrical geometry was chosen to allow the development of a thermal gradient within material, around the shear section, as during a real combustion of timber members. Furthermore, it guarantees a uniform distribution of temperature in the shear section concerned by the tests.

On Fig. 1, T₁ and T₂ represents the positions of the thermocouples used to measure the temperatures at the section in shear. Three additional thermocouples (T_{S1}, T_{S2}, T_{S3}) are positioned on the surface of the specimen.

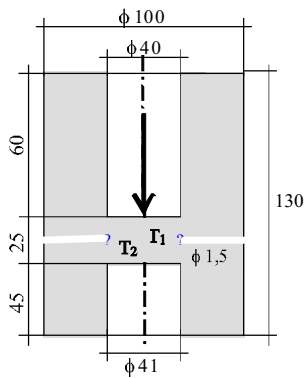


Fig. 1. Geometry of the specimen and a view after test



Fig. 2. Testing device at high temperatures

To obtain a full cutting of the shear section and a uniform distribution of stresses during test, the height of the shear section was selected using different values. This choice was operated on the basis of a numerical study based on a 2D finite element elastic model, due to the symmetry of the specimen. The finite element model was implemented in the finite element code MSC MARC [6]. So, the evolution of the stresses along a shear section of 35 mm in height show that uniform distribution of stress is already reached for a 24 mm height (Fig. 3). Thus the height of the shear section was chosen equal to 25 mm.

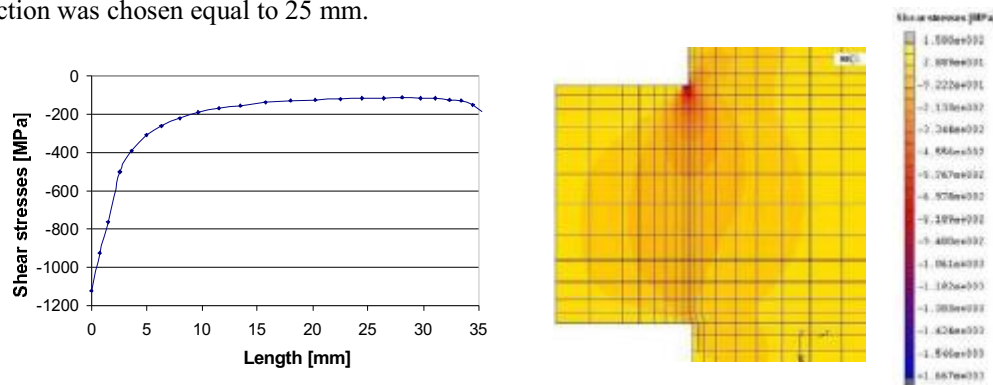


Fig. 3. Evolution of stresses along the shear section

The shear force was applied experimentally on the specimens using the test arrangement shown in Fig. 2. The wood specimens were introduced into the furnace which allowed the required temperature to be kept constant during the loading. The load is applied using a steel cylinder of diameter equal to 39,8 mm to allow its free displacement without friction inside the wood whole. On the top of the furnace, the gap between the steel cylinder and the boundary of the furnace was insulated with mineral wool to guarantee the homogeneity of the temperature inside the furnace (Fig. 2.).

2 TESTING PROGRAMM

The rate of loading of the specimens, managed by imposed displacement, was equal to 0,3 mm/min for all the tests. Four different types of tests were carried out considering the normal conditions or the fire conditions with the specimens dried or not before test with two different temperatures. The types of specimens are described hereafter.

- Tests in fire conditions:
 - Tests 1 to 4

For these four tests, the temperature of the furnace was fixed to 250°C. The loading of the specimen began when the temperature measured by the thermocouples T1 and T2 reached 100°C. This process allows obtaining a thermal gradient inside the specimen (between the surface and the shear section).

- Tests 5 and 6

For these two tests, the specimens were dried in a heating room to reach a moisture content equal to 0%. Then, the mechanical test in the furnace was conducted. The temperature of the furnace was fixed to 105°C. The loading began when the temperatures inside the specimen were stabilized to a temperature close to 100°C. Thus, the temperature inside the specimens can be considered homogeneous and constant.

- Test 7

The conditions of the test are similar to those of tests 1 to 4 but the loading begins when the temperature at the sheared section reached 150°C. The specimen is dried before the test in the same conditions as for the specimens of tests 5 and 6.

- Tests in normal conditions
 - Tests 8 and 9

These two tests are realized in cold conditions with normal room temperature (20°C) to obtain a reference.

3 TESTS RESULTS AND DISCUSSION

3.1 Thermal results

During the tests in fire conditions, three thermocouples (F₁, F₂, F₃) were used to measure the temperatures inside the furnace. Three other thermocouples were positioned on the surface of the specimen (T_{S1}, T_{S2}, T_{S3}). Finally, the thermocouples T₁ and T₂ were used to measure the temperatures at the sheared section. The values of temperature measured by these thermocouples showed the homogeneity of the temperatures around the specimen and in the shear section. An example of the measured temperatures is shown in Fig. 4. It can be observed a good correlation between the different measures and a good homogeneity of the temperatures in each zone of measurement.

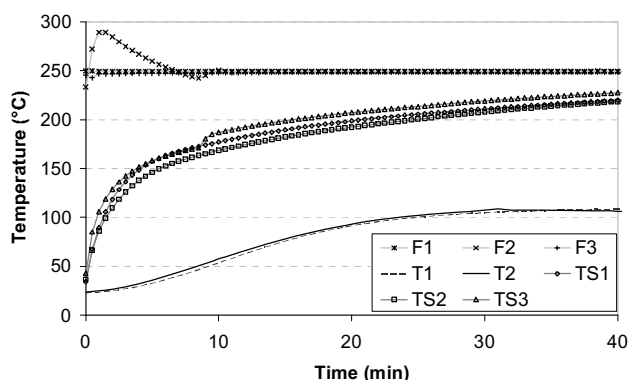


Fig. 4. Temperatures measured (furnace, specimen surface and shear section): test 2

A numerical approach of modelling of the heat transfers within the tested specimens was carried out using the recommendations of EN 1995-1-2 for the thermal properties of timber. The results of the numerical simulations (Fig. 5.) show a good approximation of the temperatures below 100°C.

Beyond this temperature, a plateau is observed on the experimental results, due to the evaporation of the water contained in wood. Besides, the use of the fictitious properties of timber provided by EN 1995-1-2 seems to not be enough to represent exactly the distribution of temperature inside the wood specimen. Thus, this difference can be explained by the fact that the numerical model does not take into account the phenomena of mass transfer within material [7]. This aspect has to be improved.

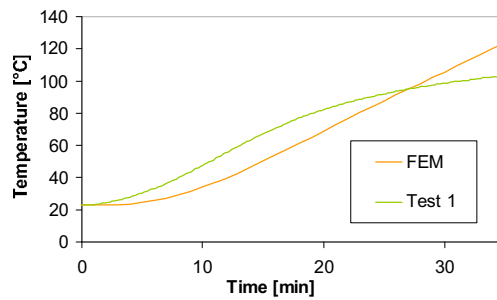


Fig. 5. Comparison between FEM and experiment (temperature)

3.2 Load-displacement results

- Tests 1 to 4 and 7

Fig. 6 shows the load-displacement curves for the tests 1-4 and 7. Fig. 7 shows the evolution of the temperature and the load versus time for test 1.

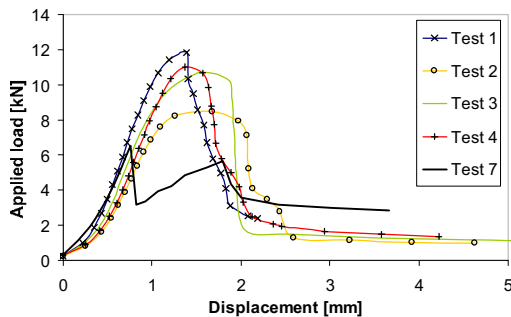


Fig. 6. Load-displacement curves (tests 1-4 and 7)

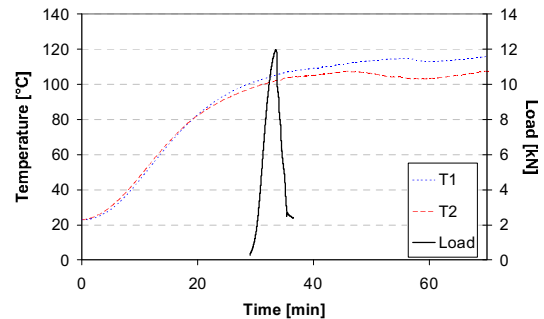


Fig. 7. (Load, temperatures)-time curves (test 1)

From Fig. 6 and 7, the following remarks can be drawn:

1. For tests 1-4, a good homogeneity of the results is obtained with the exception of the test 2 for which the value of the shear strength is weaker (Tab. 1.).

Tests	Test 1	Test 2	Test 3	Test 4
$F_{failure}$ [kN]	118,3	84,9	107,3	110

Tab. 1. Failure loads for tests 1 to 4

2. Tests (1-4) present a progressive failure of the specimens. This can be explained by the fact that the water contained in wood migrates toward the sheared section. Then, the moist fibers of wood fail gradually and increase the friction at the sheared interface. The observation of the

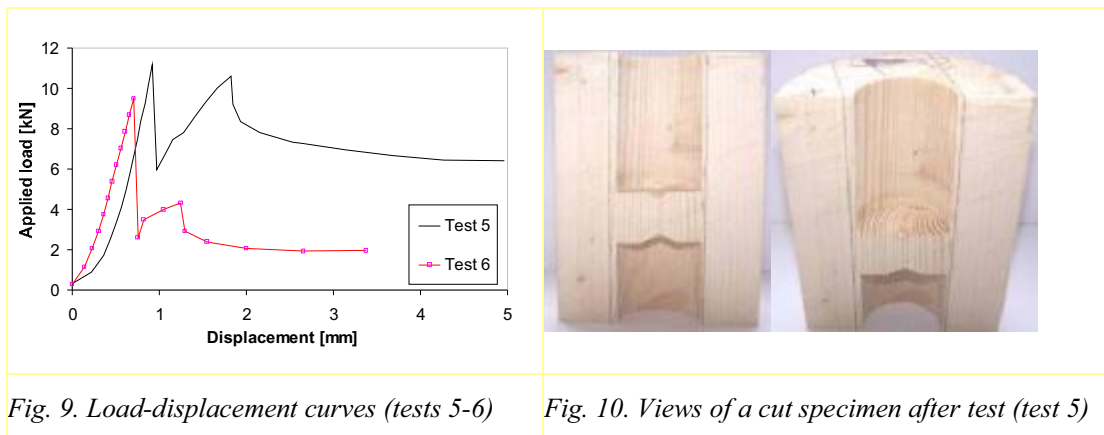
failure profile of the specimen confirms this remark (Fig. 8.). In fact, a brown colour is observed inside specimens 1-4, due to the migration of water against the steel cylinder, and the visible failure surface is not smooth.



Fig.8. View of a cut of specimen 3 after the test

3. A decrease of the shear strength of about 40% is observed for the test 7, realised at 150°C, in comparison with the values of tests 1-4 realised at 100°C.
 4. The load-displacement curve for test 7 is appreciably different from that of tests 1-4. It can be observed a first brittle failure and then a second at a weaker level of strength. Thus, the absence of water inside the material seems to be influencing the failure mode. This observation is confirmed by the results of tests 5-6.
- Tests 5-6

Fig. 9 shows the load-displacement curves for the tests 5 and 6, realised at 100°C with dried specimens.



The observation of the specimen after the test shows that the failure profile is different (Fig. 10.). In fact, the brown colour observed with tests 1 to 4 does not appear in the case of the dried specimen. It can be observed a clear and smooth failure surface at the sheared section.

Fig. 9 shows that the moisture content of wood doesn't affect the shear strength of specimens. The same strength is obtained for tests 1 to 4 (2,8 to 3,8 MPa). It appears that the wood moisture content does not affect the strength but the presence of water within material changes the failure mode of tested specimens. However, it should be noted that the initial moisture content of the specimen was relatively weak (8%). This observation will have to be confirmed later with other tests carried out on specimens having higher moisture content (12%).

- Cold tests 8-9

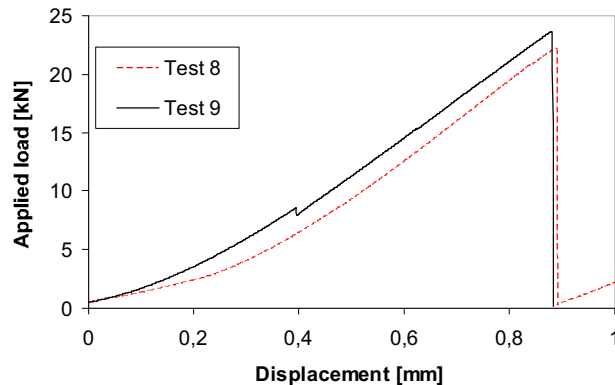


Fig. 11. Load-displacement curves (tests 8 and 9)

A low dispersion is obtained with the two tests in cold conditions (Fig. 11). The comparison of the strength values at high temperature with those given by cold tests, shows that the shear strength at 100°C decreases by 40 to 50%. At 150°C, this resistance is reduced by 65% (only one value from test 7).

3.3 Comparison with the results of Eurocode 5

The values of strength obtained by tests in fire conditions are compared with those given by the reduction factors provided by EN 1995-1-2 (Fig. 12.). It can be observed a good agreement between the experimental results and the values of Eurocode.

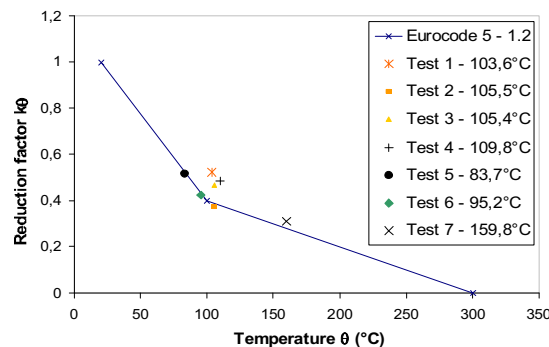


Fig. 12. Reduction factors of the shear strength (tests and EC5)

CONCLUSIONS

The present study presented shear results to be used in the thermo-mechanical modelling of timber connections. Some tests were carried out to study the shear behaviour of glued laminated timber at high temperatures. These tests were performed using specimens with a specific cylindrical geometry to reproduce various experimental conditions. Four different types of tests were performed. The results of these tests show that the moisture content of the material does not affect the shear strength, but influences the failure mode. It appears in fact that the moist fibers of wood fail gradually. These results, obtained with a limited number of tests, realized on specimens with

weak moisture content (8 %), must be confirmed by additional tests which allow analyzing the effects of higher moisture contents of wood specimens.

For fire design of timber connections, it is necessary to know the decrease of shear strength with the increase of temperature. At 100°C, the obtained results show that the shear strength of the tested specimens decreases by 40 to 50%. At 150°C, the decrease is about 65%. These reduction factors are comparing with the values given by Eurocode 5-1-2. Homogeneous results and a good agreement between experimental results and Eurocode values are obtained. The results of this study show that the reduction factor for shear strength of parallel to grain of softwood, given by Eurocode 5-1-2, is valid for the glulam in strength class GL24h. The geometry of the specimens selected for the shear tests appears as relevant for the study.

As further developments, the preliminary results obtained by this study will be confronted with the results of another experimental campaign, realized on a larger number of specimens with the same geometry but different moisture contents. The final aim of this research work is to integrate the shear properties of wood into a modelling of thermo-mechanical behaviour of dowelled timber connections [8].

REFERENCES

- [1] Buchanan A. H., Structural design for fire safety, *John Wiley & Sons, ISBN 0471 89060 X, 421 pages*, 2004
- [2] König J., Effective thermal actions and thermal properties of timber members in natural fires, *Journal of Fire and Materials, Vol. 30, pp. 51-63*, 2005
- [3] König J., Structural fire design according to Eurocode 5 – Design rules and their background, *Journal of Fire and Materials, Vol. 29, pp. 147-163*, 2004
- [4] EN1995-1-2, Design of timber structures – General rules Structural fire design”, *CEN TC250-SC5*, Brussels, 2004
- [5] NF P 21-400, Structural timber and wood-based products - resistance classes and related permissible stresses, *pp. 21-400*, 2003
- [6] MSC.Software Corporation, MSC.Marc, User Manual, A: theory and user information, 2005
- [7] Fredlund B., Modelling of Heat and Mass Transfer in Wood Structures During Fire, *Fire Safety Journal 0379-7112/92/\$05-00*, 1992
- [8] Audebert M., Bouchaïr A., Dhima D., Taazount M., Modelling of the behaviour of timber joints in fire, 24th *Civil Engineering University meetings*, Nancy, France, 2008 [In French].

TIMBER CONNECTIONS UNDER FIRE LOADING

A component model for numerical modelling

Paulo Cachim ^a, Jean-Marc Franssen ^b

^a University of Aveiro/LABEST, Department of Civil Engineering, Aveiro, Portugal

^b University of Liege, Department of Structural Engineering, Liege, Belgium

INTRODUCTION

Connections are key elements in structures. Consequently, understanding the behaviour of the connections is fundamental for an adequate modelling of structures, because the load-deformation behaviour of the connections will influence the overall stress distribution in the structure. Timber connections are usually considered in analysis either as fully rigid or fully hinged, however, only the use of a semi-rigid behaviour will allow a more realistic structural modelling.

For the design at room temperatures, the current design methodology of many codes, e.g. EC 5 [1], is based on a plastic limit state design that allows the calculation of the ultimate load bearing capacity of the connections. However, only a simple expression that is function only of the timber density and fastener diameter is proposed for the load-slip characterization of the connections. This expression doesn't consider some effects, such as the load to grain angle or the geometry of the connection, that are fundamental for an accurate modelling of timber connections.

The goal of this paper is the development of a simple component model for the behaviour of dowelled timber connections under fire loading. In order to reach this goal, constitutive models were implemented for room and fire temperatures. Finite element simulations were performed using a finite element code for structural analysis under fire loading and EC 5 values and experimental data were used to calibrate the model.

1 THE COMPONENT MODEL FOR TIMBER CONNECTIONS

The component model considers the connection as an assembly of individual components. Once the individual constitutive components are identified and characterized, the overall behaviour of the connection can be obtained through the so-called assembly procedures. Each of the components behaves in a way that is independent of the other components, of the connection layout and of the loading type. Therefore, each component can be modelled separately, with its own stiffness and strength. When the connection is loaded, the distribution of forces in the connection is determined by the relative stiffness/strength and by the position of the individual components. Application of the component model to timber connections requires the knowledge of the behaviour of all individual components of the timber connection. For a dowel type connection with a single fastener, a timber component and a dowel component can be identified.

The behaviour of the timber component can be determined by embedding tests that relate the force applied to a fastener to the corresponding embedding in timber. The dowel component is represented as a beam model. The materially non linear behaviour of the section can be captured if the section is discretized by a fibre model. The components can be assembled into the connection model. Fig. 1 shows the case of a fastener in double shear. A typical finite element modelling of the component model of the connection uses a series of beam elements

to discretize the dowel with a spring connected at each node and representing the behaviour of the timber.

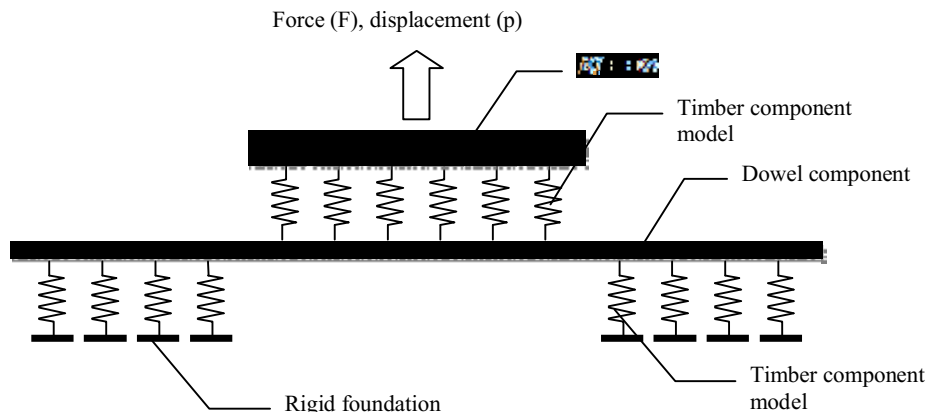


Fig. 1. Model of a single fastener connection

2 PARAMETERS OF THE MODEL AT ROOM TEMPERATURE

All parameters of the model should ideally be determined experimentally. However, in this paper, the available formulas presented in EC 5 are used, complemented by additional information obtained from available experimental data to derive generic properties of the timber component.

The general constitutive model for the timber component is shown in Fig. 2 on which the relevant parameters are indicated. The parameters are mainly dependent of the force to grain direction, α . A total of four parameters are necessary to completely define the model, for each α value, but, by using the well-known Hankinson expression, a property value at an angle α to the grain can be obtained from the parallel (subscript 0) and perpendicular (subscript 90) to grain directions.

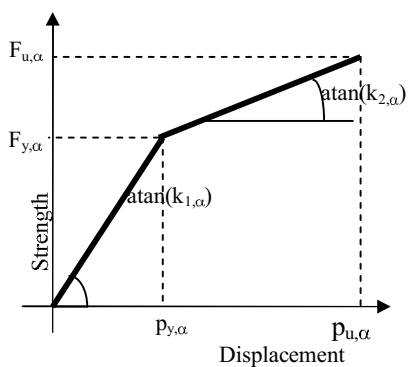


Fig. 2. Idealized force displacement curve for dowel-timber interaction

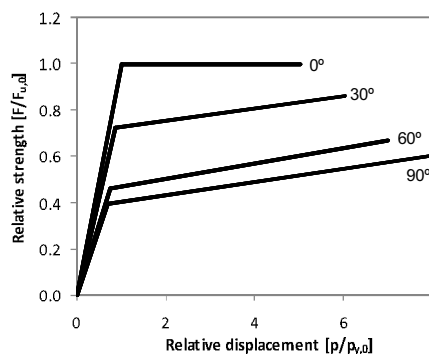


Fig. 3. Relative strength-relative displacement curves for 0, 30, 60 and 90°

The ultimate strength for dowels or bolt fasteners, $F_{u,\alpha}$, is derived from EC5 [1] expressions for dowel-type bolts as

$$F_{u,\alpha} = f_{h,\alpha} d = \frac{f_{h,0} d}{k_{90} \sin^2 \alpha + \cos^2 \alpha}, \quad k_{90} = 1.35 + 0.015d \quad (1)$$

where d is the fastener diameter in mm and $f_{h,\alpha}$ is the embedding strength at an angle α to the grain, $f_{h,0}$ is the embedding strength parallel to grain and k_{90} is the parallel/perpendicular embedding strength ratio ($f_{h,0} / f_{h,90}$). When no experimental data is available for $f_{h,0}$ and $f_{h,90}$, $F_{u,\alpha}$ can be obtained using the EC5 embedding strength for dowels expression:

$$F_{u,\alpha} = \frac{F_{u,0}}{k_{90} \sin^2 \alpha + \cos^2 \alpha} = \frac{0.082(1 - 0.01d) \rho_k d}{k_{90} \sin^2 \alpha + \cos^2 \alpha} \quad (2)$$

where d is in mm and ρ_k is the timber density in kg/m³. The yield strength, $F_{y,\alpha}$, can be related to the ultimate strength by multiplying the latter by $F_{y,\alpha} = \eta_\alpha F_{u,\alpha}$. Experimental results [2, 3] show that $\eta_0 = 1.0$ and that η_{90} ranges from 0.5 to 0.8 (an average value of 0.65 is recommended in absence of experimental data). By knowing the values η_0 and η_{90} it is possible to calculate $F_{y,0}$ and $F_{y,90}$ and with help of Hankinson equation the value $F_{y,\alpha}$ can be related to $F_{u,0}$ as:

$$F_{y,\alpha} = \frac{\eta_0}{\frac{\eta_0}{\eta_{90}} k_{90} \sin^2 \alpha + \cos^2 \alpha} F_{u,0} \quad (3)$$

The expression for η_α as a function of η_0 and η_{90} finally reads

$$\eta_\alpha = \frac{F_{y,\alpha}}{F_{u,\alpha}} = \frac{k_{90} \sin^2 \alpha + \cos^2 \alpha}{n_{90} k_{90} \sin^2 \alpha + \cos^2 \alpha} \eta_0, \quad n_{90} = \eta_0 / \eta_{90}. \quad (4)$$

The values for the yield displacement, $p_{y,\alpha}$, must be determined from available experimental results. Lam [2] stated that stiffness is independent of the dowel diameter (diameters of tested dowels ranged from 10 to 20 mm). Using again the results of [2, 3], the displacement $p_{y,0}$ can be described by the following proposed expression

$$p_{y,0} = 0.1(1 - 0.01d)d \quad (5)$$

Using the fact that $\eta_0 = 1$, the value $k_{1,0}$ can be calculated using EC 5 expression as:

$$k_{1,0} = \frac{F_{y,0}}{p_{y,0}} = 0.82 \eta_0 \rho_k = 0.82 \rho_k \quad (6)$$

The stiffness $k_{1,90}$ can be assumed to be related to the stiffness $k_{1,0}$ by a factor ζ_{90} as $k_{1,90} = \zeta_{90} k_{1,0}$. Experimental data shows ζ_{90} in the range 1.5 to 2.0 and, for analysis purposes, in the absence of experimental data, can be estimated as $\zeta_{90} = 1.8$. The value $k_{1,\alpha}$ then reads

$$k_{1,\alpha} = \frac{k_{1,0}}{\zeta_{90} \sin^2 \alpha + \cos^2 \alpha} \quad (7)$$

From Fig. 2 and using previous equations, the yield displacement $p_{y,\alpha}$ is given by

$$p_{y,\alpha} = \frac{F_{y,\alpha}}{k_{1,\alpha}} = \frac{\zeta_{90} \sin^2 \alpha + \cos^2 \alpha}{n_{90} k_{90} \sin^2 \alpha + \cos^2 \alpha} p_{y,0} \quad (8)$$

There is, to our knowledge, no reliable information about the ultimate displacements p_u . In fact, the embedding strength tests performed according to EN 383 stop at an ultimate displacement of 5 mm. However, experimental results indicate that timber continues to sustain load beyond this value, especially for loads applied perpendicular to the grain. In the

absence of more consistent data, the values of $p_{u,0} = 5$ mm and $p_{u,90} = 8$ mm are suggested. The ultimate stiffness $k_{2,\alpha}$ then reads

$$k_{2,\alpha} = \frac{F_{u,\alpha} - F_{y,\alpha}}{p_{u,\alpha} - p_{y,\alpha}} \quad (9)$$

Fig. 3 shows the relative strength-relative displacement curves for $\alpha = 0, 30, 60$ and 90° obtained with the proposed model using default values for $n_{90}, \zeta_{90}, p_{u,0}$ and $p_{u,90}$.

3 PARAMETERS OF THE MODEL AT ELEVATED TEMPERATURES

A two-step approach is used for the component model for timber connections under fire loading. Initially, a three-dimensional thermal analysis of the connection is carried out that allows the determination of the temperature field in fasteners and timber. Afterwards, the component model previously described for the connection is used to determine the mechanical behaviour of the connection. The three-dimensional thermal analyses of the connections were carried out using program SAFIR [4] with material thermal properties defined in Eurocodes.

The determination of the mechanical parameters for the timber component at elevated temperatures was based on the reduced mechanical properties at elevated temperatures proposed in the structural fire design part of EC 5 [5]. Since shear fasteners in timber connections work by compressing the timber, the reduction factors for compressive stiffness and strength were adopted for the timber component. By applying these factors for material properties described previously, the strength-displacement curves of the timber component at elevated temperatures can be obtained. The ultimate displacement was kept independent of temperature. Examples of these curves at selected temperatures are shown in **Erro! A origem da referência não foi encontrada.**

The non linear mechanical properties at elevated temperature for the dowels are obtained from recommendations of EC 3 [6].

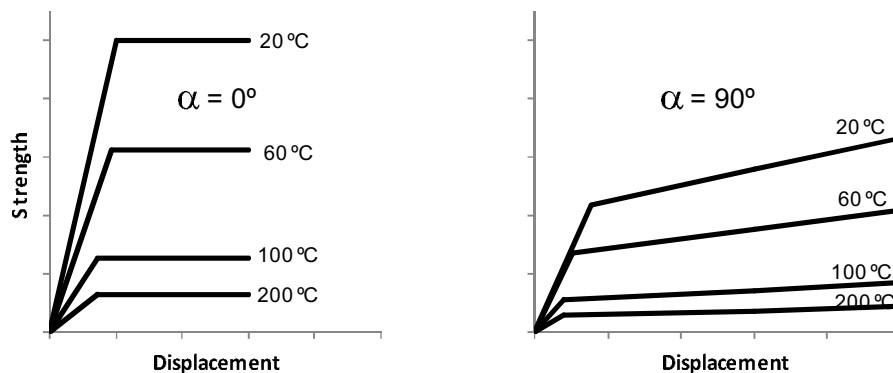


Fig. 4. Relative strength-displacement curves at selected temperatures for $\alpha = 0^\circ$ and 90° .

4 MODEL PERFORMANCE UNDER FIRE CONDITIONS

The model performance under fire conditions was compared with experimental tests with dowels and bolts. The results used for comparison purposes were those from Laplanche *et al.* [7] and Kruppa *et al.* [8]. Summary of side member thickness, fastener type, applied load level and time to failure are presented in Table 1. In dowelled connections, some of the dowels (usually one in four) were replaced by bolts to prevent separation of members during fire tests.

The methodology used for the analysis of fire resistance was as previously described: first a thermal analysis is performed and then obtained temperatures are applied in the mechanical model. Numerical simulations were carried out using a single fastener, since the effect of the number of fasteners for the calculation of the load ratio-time to failure curves is very small and, as a consequence, the use of a single dowel should provide similar results.

Table 1. Summary of experimental and numerical test results

Author	Type	Thickness		Fastener diameter [mm]	Number of fasteners [dowel+bolt]	Load ratio [%]	Time to failure			
		Side [mm]	Center [mm]				Experimental [min]	Numerical [min]	Deviation [min]	Error [%]
Laplanche <i>et al.</i> [7]	Dowel	84	160	16	6+2	29.9	54	48	-6	-11.1
						9.9	79	76	-3	-3.8
	Dowel	64	112	16	6+2	30.1	41	35	-6	-14.6
						30.0	38	35	-3	-7.9
						20.0	46	42	-4	-8.7
						19.8	45	42	-3	-6.7
Kruppa <i>et al.</i> [8]	Dowel	50	80	12	6+2	56.0	13	16	3	23.1
						28.0	32	26	-6	-18.8
	Dowel	60	100	20	6+2	65.0	7	20	-	-
						33.0	35	30	-5	-14.3
					12+4	62.0	22	20	-2	-9.1
						31.0	41	31	-10	-24.4
Bolt	50	80	12	0+8	42.0	23	26	3	13	
					21.0	38	38	0	0	
Bolt	60	100	20	0+8	57.0	13	11	-2	-15.4	
					24.0	22	20	-2	-9.1	
Bolt	60	100	20	0+8	59.0	15	17	2	13.3	
					30.0	24	25	1	4.2	

Numerical results obtained with the component model and deviations to experimental results are also presented in the last columns of Table 1. Ignoring the case of dowels loaded at a load ratio of 65 % that fail after 7 min and for which there should be some problem in the tests (according to [8]) the absolute average error for the time to failure is 3.55 min and the standard deviation is 2.33 min. It can be seen that a good agreement was found between the numerical and experimental results both for the case of dowels and bolts.

5 CONCLUSIONS

A component model for dowelled type timber connections subjected to fire has been developed. A generic constitutive model for the timber component can be defined with two parameters, namely the timber density and the dowel diameter. The constitutive model was calibrated with available experimental embedding tests. The component model showed good accuracy when used in several types of connections and compared with experimental results collected from two different sources.

When applied to timber connections under fire loading, the component model showed interesting possibilities, allowing the identification and characterization of the main mechanisms of the connection behaviour, indicating that regardless of its simplicity the model is quite capable of modelling the load-deformation behaviour of connections at room temperature and under fire conditions.

REFERENCES

- [1] EN 1995-1-1:2004. Eurocode 5: Design of timber structures - Part 1-1: General - Common rules and rules for buildings. CEN, Belgium.
- [2] Lam LY. Développement de modèles analytiques pour la prédiction du comportement élastique des assemblages mécaniques à broches dans la construction en bois (in French), PhD dissertation, University of Liege, Belgium, 2006.
- [3] Pederson MU. Dowel Type Timber Connections – Strength Modelling, PhD dissertation, Rapport BYG·DTU R-039, Technical University of Denmark, Denmark, 2002.
- [4] Franssen J-M. SAFIR. A Thermal/Structural Program Modelling Structures under Fire, Engineering Journal, A.I.S.C., 2005: 42 (3), pp. 143-158.
- [5] EN 1995-1-2:2004. Eurocode 5: Design of timber structures - Part 1-2: General - Structural fire design. CEN, 2004.
- [6] EN 1993-1-2: 2005. Eurocode 3: Design of steel structures – Part 1-2: General rules - Structural fire design. CEN, 2005.
- [7] Laplanche, K., Dhima, D. & Racher, P. 2004. Predicting the behaviour of dowelled connections in fire: Fire test results and heat transfer modelling. 8th World Conference on Timber Engineering, WCTE 2004, Lahti Finland
- [8] Kruppa, J., Lamadon, T. & Racher, P. 2000. Fire resistance tests of timber connections. CTICM, INC-00/187-JK/NB..

EVALUATION OF NATURAL AND PARAMETRIC TEMPERATURE-TIME CURVES FOR THE FIRE DESIGN OF CROSS-LAMINATED WOOD SLABS

Kathinka Leikanger Friquin

National University of Science and Technology, Dept. of Civil and Transport Engineering, Trondheim, Norway

1 INTRODUCTION

Many temperature-time curves for performance-based fire design have been developed, but most of them are only applicable to concrete, brick, lightweight concrete and steel structures. As most of the methods for determining the temperature-time development in a fire compartment only include the fire load of the furniture and other contents in the fire compartment, few of the temperature-time curves developed give a correct picture of the temperature development in a compartment surrounded by combustible wooden structures. The contributions made to the fire load by the wooden boundaries and structures are very often ignored, resulting in an optimistic temperature development. In the present article, temperature-time curves found in the literature for complete fires, including growth stage, flashover, fully developed fire and decay stage, have been evaluated based on their ability to describe the temperature development in compartments with boundaries of cross-laminated slabs, their applicability and suitability to these types of structures. Four models for determining temperature-time curves that might be applicable to wooden structures were found. The project is funded by the Norwegian Research Council.

1 DESCRIPTION OF TEMPERATURE-TIME CURVES FOR WOODEN STRUCTURES

As many of the temperature-time curves for fires in compartments are developed mainly for testing and design of non-combustible structures, such as concrete and steel, the applicability of these curves to wooden structures must be evaluated. There are a few different types of wooden structures, like light frame walls, glue-laminated structures with insulation and plasterboards between the columns, fully exposed glue-laminated structures, and partly or fully exposed cross-laminated slabs. The different structures will give different temperature-time curves, and the charring rate may vary. In this paper only cross-laminated slabs have been considered. The curves consider various parameters, and for wooden structures the important parameters might be different from steel and concrete structures. The applicability to wooden structures therefore has to be considered for each and every temperature-time curve.

1.1 The “Swedish curves”

Magnusson and Thelandersson [1] developed temperature-time curves describing all stages of the fire (growth, flashover, fully developed and decay/cooling) for seven different compartments, designated A-G, based on their bounding surfaces, see *Fig. 1*. Curves for compartments with wooden boundaries are not developed. The curves are developed based on the fire load density (MJ/m^2 of bounding surface area), the area and height of the ventilation openings, the thermal properties of the bounding surfaces, and the heat balance in the compartment, i.e. heat transfer through the structures bounding the enclosed space, radiation through the openings, and the replacement of combustion gases by cold air. *Fig. 1* below shows temperature-time curves for compartment A with opening factors 0.04 and 0.08 $\text{m}^{1/2}$, and various fire loads.

The curves developed by Magnusson and Thelandersson [1] are based upon a few assumptions:

- The temperature in the interior of the whole enclosed space is uniform at any given instant.
- The coefficient of heat transfer to the interior bounding surfaces of the enclosed space is uniform at every point.
- The heat flow through the bounding structures of the enclosed space is one-dimensional and, except for the window and door openings, if any, uniformly distributed.

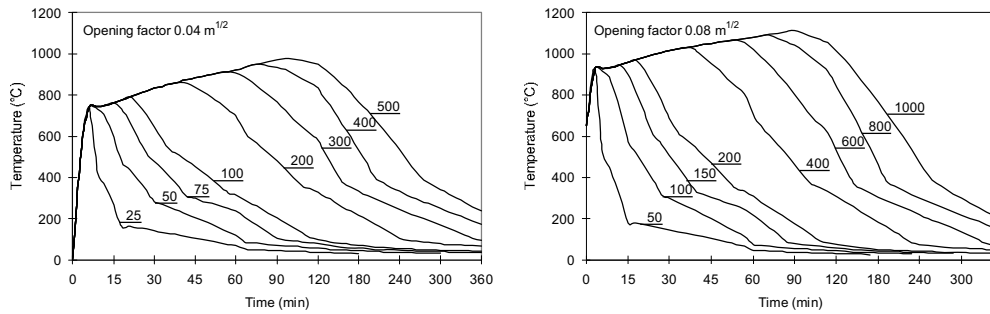


Fig. 1. Temperature-time curves for a complete fire developed by , for compartment A with opening factors 0.04 and 0.08 m^{1/2}. The numbers on each curve are the fire load densities distributed on the total surface area.

Pettersson and Ödeen [2] developed correction factors, k_{fict} , to convert the curves for the standard compartment A into curves for the other defined compartments. The correction factors range from 1.0, for bounding surfaces with thermal properties averaging between concrete, brick and lightweight concrete, to 3.0, for steel sheets and mineral wool. The correction factors are based upon thermal differences in the bounding surfaces of the compartments. Magnusson and Thelandersson [1] did not calculate curves for compartments with wooden boundaries, and Pettersson and Ödeen [2] did not calculate correction factors for such compartments. However, according to König et al. [3] the correction factors can be calculated based on the thermal properties of the boundaries of the compartments, as given in Eq. (1):

$$k_{fict} = \frac{1160}{\sqrt{\lambda \rho c}} \quad (1)$$

where λ is the thermal conductivity of the enclosure [W/mK], ρ is the density of the enclosure [kg/m³] and c is the specific heat of the enclosure [J/kgK]. For a fire compartment with uniform boundaries of cross-laminated wooden elements of pine or spruce typically used in Scandinavia, with density 500 kg/m³, specific heat 1900 J/kgK, and thermal conductivity 0.12 W/mK, the correction factor k_{fict} will therefore be 3.44. Procedure:

1. Calculate the opening factor, O :

$$O = A_v \sqrt{h} / A_t \quad (2)$$

where A_v is the total area of vertical openings on all walls [m²], A_t the total area of the enclosure (walls, ceiling and floor, including openings) [m²], and h the weighted average of window heights on all walls [m].

2. Determine the fire load density, $q_{t,d}$ (fire load density per unit total surface area):

$$q_{t,d} = \Sigma(M_{k,i} \cdot H_{ui} \cdot m) / A_t \quad [\text{MJ/m}^2] \quad (3)$$

where $M_{k,i}$ is the amount of the combustible material i in the compartment [kg], H_{ui} the net calorific value of material i [MJ/kg], m the combustion factor, and A_t the total area of the enclosure (walls, ceiling and floor, including openings) [m²].

3. Calculate the correction factor, k_{fict} , as given in Eq. 1.

4. Find corrected opening factor, O_{fict} , and fire load density, $q_{t,d,fict}$ by multiplying O and $q_{t,d}$ with k_{fict} .

5. Find the curve for compartment A with O_{fict} and $q_{t,d,fict}$ and use it as the temperature-time curve for the fire. For fire compartments with O_{fict} and $q_{t,d,fict}$ other than those found in the curves, interpolation can be used to determine the temperature-time development.

The curves can be found in Magnusson and Thelandersson [1] and Pettersson and Ödeen [2].

1.2 EN 1991-1-2 Standard temperature-time curve

The standard temperature-time curve in [4] is given by:

$$\theta_g = 20 + 345 \log_{10}(8t + 1) \quad (4)$$

where θ_g is the gas temperature in the fire compartment [°C] and t the time [min].

In Sweden a cooling rate of 10°C/min has been used.

1.3 EN 1991-1-2 Parametric temperature-time curve

The procedure to calculate a temperature-time curve based on EN 1991-1-2 [4] is as follows:

1. Calculate temperature-time curve for the heating stage, found in EN 1991-1-2 Annex A(3):

$$\theta_g = 20 + 1325 (1 - 0.324e^{-0.2t^*} - 0.0204e^{-1.7t^*} - 0.472e^{-19t^*}) \quad (5)$$

where θ_g is the gas temperature in the compartment [°C]. The gas temperature is a function of time, opening factor, and thermal properties (density, specific heat and thermal conductivity) of the boundary of the compartment.

2. Calculate the maximum temperature, θ_{max} , in the heating stage using EN 1991-1-2 Annex A(7). If $t_{max} = t_{lim}$ the fire is fuel controlled, and if $t_{max} > t_{lim}$ the fire is ventilation controlled.

3. The cooling stage of the fire is calculated based on the maximum temperature, θ_{max} , the opening factor, O , the product of the density and thermal properties, b, t_{max}^* , and a factor x , which express whether the fire is fuel controlled or ventilation controlled. Three different equations describe the cooling stage, based on the duration of the fire. The cooling stage is a function of time, opening factor, and thermal properties of the boundary of the compartment.

1.4 iBMB parametric fire curve

The iBMB parametric fire model is described by Zehfuss and Hosser [5] and Zehfuss [6] as a model that considers the actual boundary conditions of the fire compartment concerning fire load, ventilation conditions, geometry and thermal properties of the enclosure. The parametric equations for the temperature-time curve were developed for a reference fire load density of $q'' = 1300 \text{ MJ/m}^2$ (upper value for residential and office buildings). The procedure when determining iBMB parametric fire curves:

1. Calculate opening factor O , fire load density q , total fire load Q , averaged thermal property of the boundaries, total area of boundaries incl. openings A_i , total area of boundaries excl. openings A_T .

2. Calculate the maximum rate of heat release $\dot{Q}_{max} = \min[\dot{Q}_{max,v}; \dot{Q}_{max,f}]$ and determine whether the fire is ventilation or fuel controlled during the fully developed fire stage.

3. The curves have three distinct points at the times t_1 , t_2 and t_3 , where the slope of the curves changes, see *Fig. 2*. Growth stage: From the initiation of the fire until t_1 , the RHR rises quadratically, $\dot{Q}(t) = \dot{Q}_0 (t/t_g)^2 [\text{MW}]$, where $\dot{Q}_0 = 1 \text{ MW}$ and $t_g = 300 \text{ s}$ (for residential and office buildings). The upper layer temperature increases rapidly at this stage. Fully developed fire: At t_1 the RHR has reached its maximum, \dot{Q}_{max} , and remains constant until t_2 . Between t_1 and t_2 the upper layer temperatures increases moderately, reaching its maximum at t_2 . Cooling stage: 70% of the fuel is consumed at t_2 and the RHR drops off linearly, at the same time the upper layer temperature starts to decline. At t_3 the total fire load is consumed and the RHR decreases to 0, and the upper layer temperature-time curve bends and declines slower than before. The times t_1 , t_2 and t_3 must be calculated for both the maximum fire load density, q'' , for the actual building category, and the actual fire load density for the specific compartment, q''_x . The first point, t_1 , is common for both fire load densities. For fire load densities less than the maximum q'' , the maximum temperature is achieved accordingly earlier, see *Fig. 2*.

4. The temperatures T_1 , T_2 and T_3 for the maximum fire load density of $q'' = 1300 \text{ MJ/m}^2$ can be calculated based on the RHR curve, and the temperature-time curve can be calculated based on the

parametric equations for ventilation or fuel controlled fires, according to the results from bullet No. 2 above. The equations are given in [5,6].

5. When the temperature-time curve for the maximum fire load density q'' is drawn, the temperatures $T_{2,x}$ and $T_{3,x}$ can be found. $T_{2,x}$ is found on the curve at time $t_{2,x}$. $T_{3,x}$ is found on the $T_{3,x}$ Log₁₀-curve described by $T_{3,x} = (T_3 / \log_{10}(t_3 + 1)) \cdot \log_{10}(t_{3,x} + 1)$ at time $t_{3,x}$. The temperature-time curve for a fire compartment with a fire load density $q'' \leq 1300 \text{ MJ/m}^2$ can now be drawn based on the parametric equations given in [5,6].

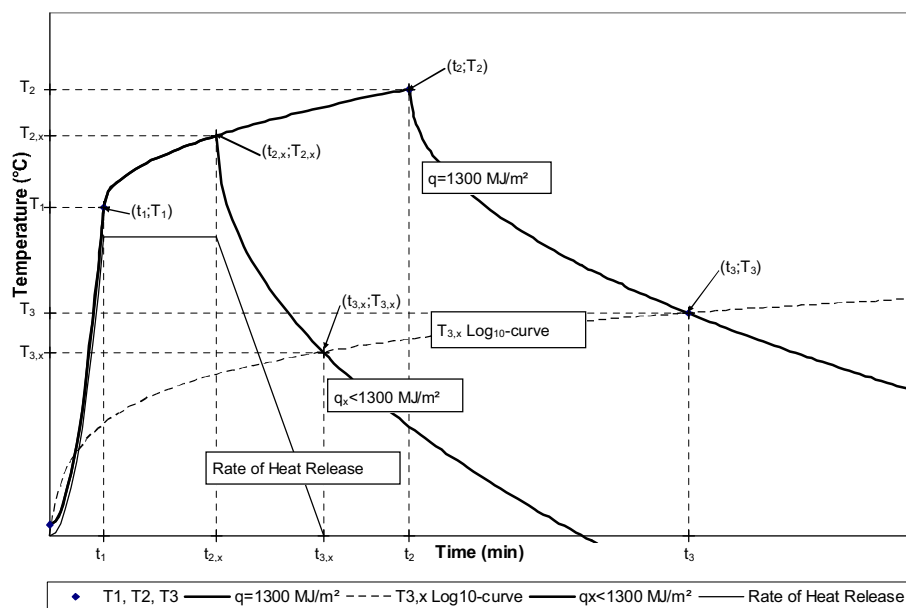


Fig. 2. Determination of the temperatures $T_{2,x}$ and $T_{3,x}$. Rate of Heat Release and temperature-time curve for $q < 1300 \text{ MJ/m}^2$, and the temperature-time curve for $q = 1300 \text{ MJ/m}^2$. $T_{3,x}$ Log₁₀-curve for determination of $T_{3,x}$.

The trend of some of the curves described in this paper is shown in Fig. 3.

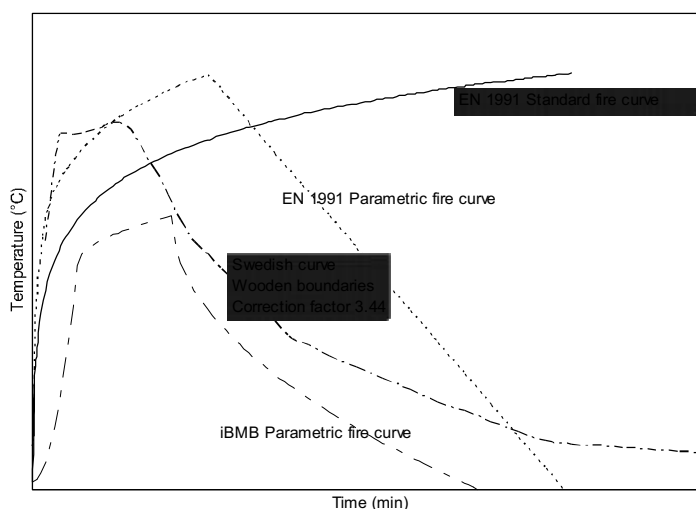


Fig. 3. The typical trend of some of the temperature-time curves described; EN 1991-1-2 Standard fire curve and Parametric fire curve, “Swedish fire curve”, and iBMB Parametric fire curve. The curves are not to scale with each other.

2 SUMMARY AND DISCUSSIONS

The models and curves described above have been evaluated based on their ability to describe the temperature development in compartments with boundaries of cross-laminated slabs, their applicability and suitability to these types of structures. Five models for determining temperature-time curves that might be applicable to wooden structures were found. Most of the curves are initially developed for testing and design of non-combustible structures, but have later also been assigned for combustible structures. Experimental research, performed through the years by various laboratories, has shown that the accuracy of the temperature-time development compared to real fires is not always good. And from time to time new models for determination of temperature-time curves are developed. It is therefore necessary to study the various models and determine which ones are more applicable to wooden structures.

2.1 The “Swedish curves”

Magnusson and Thelandersson [1] and Pettersson and Ödeen [2] have not given correction factors for fire compartments with wooden boundaries, but König et al. [3] describes how to calculate the correction factor for compartments with boundaries of various thermal properties. For a compartment with exposed cross-laminated slabs on all surfaces, the correction factor was here calculated to be 3.44. This correction factor considers the thermal properties of the boundaries, i.e. the density, the thermal conductivity and the specific heat capacity of the material. The charring rate and fire load of the boundary material is not considered. It might be reasonable to first determine the temperature-time curve only based on the fire load of the inventory to find the fire duration, and then add the fire load from the boundaries calculated based on the nominal charring rate from EN 1991-1-2 and the fire duration first found. A new curve can then be found based on the new fire load density and the old opening factor. The assumptions made when developing the method simplify the curves considerably.

2.2 EN 1991-1-2 Standard temperature-time curve

The development of the fire is very dependant on the type of building you are designing. The standard temperature-time curve given by EN 1991-1-2 [4] is very conservative for slow growing fires, less so for medium growth fires and only a little for fast growing fires. The curve only describes the heating stage, and does not consider the boundary conditions or the fire load density. A cooling stage of 10°C/min has been used in Sweden, but the real cooling stage for combustible structure is not linear.

2.3 EN 1991-1-2 Parametric fire

There are many limitations to the use of the parametric fire curve given by EN 1991-1-2 [4]. For example, the maximum floor area is 500 m², maximum compartment height 4 m, thermal properties $b = \sqrt{\rho c \lambda}$ between 100 and 2200 J/m²s^{1/2}K, and opening factor between 0.02 and 0.20. To incorporate the charring of the structure, the maximum fire duration is 120 min, with a maximum char depth of 1/4 of the height or width of the structural member. The thermal properties can be taken at ambient temperature, but for most materials these properties are strongly temperature dependant. The fire load density is calculated based on the combustible inventory in the compartment and “the relevant combustible parts of the construction, including linings and finishing. Combustible parts of the construction which do not char during the fire need not to be taken into account” [4]. The “relevant combustible parts of the construction” can only be found when we know the development of the fire, which in turn can only be found when we know the total fire load density. Through iterations the temperature-time development and the contribution from the construction to the fire load density can be found.

2.4 iBMB model

The iBMB parametric fire curves can be used to determine the occurrence of flashover, breakage of windows with additional ventilation, a failure of the enclosure with loss of compartmentation, or the effect of fire fighting and sprinkler systems. The connection between the design fire and the parametric fire curve makes it possible to consider all events influencing on the natural fire and resulting in a variation of the RHR.

Experiments performed by Hakkarainen [7] show that the temperature-time curve for a small compartment with exposed heavy timber structures a relatively small opening factor can have a plateau at a relatively low temperature due to insufficient ventilation. As much as 50% of the pyrolysis gases burnt outside the compartment. When most of the movable fire load has burnt, the temperature might increase as the generation of pyrolysis gases decrease, allowing more oxygen into the compartment. None of the curves above show this phenomenon.

2 CONCLUSIONS

Four temperature-time curves have been evaluated based on their applicability to exposed wooden structures. Based on the evaluation of the temperature-time curves, the following conclusions can be drawn:

1. The geometry of the compartment, and the position and size of the ventilation openings will have a great effect on the temperature, flashover and decay stage of the fire.
2. Many of the curves have growth rates much higher than real fires.
3. Linear cooling stages are not realistic. Fire curves with linear cooling stage give too fast cooling for compartments with large surfaces of exposed wooden structure.
4. None of the curves include the fire load from the structure directly. Iterations have to be made to incorporate this contribution to the fire.
5. Assumptions can be made to determine a relevant part of the structure to be part of the fire load.
6. The “Swedish curves” and the iBMB curves resemble a real fire in a compartment with exposed wooden structures most.

Using a realistic fire development and determining the overall structural behaviour can lead to an efficient and aesthetical construction.

3 REFERENCES

- [1] Magnusson, S. E. and Thelandersson, Sven. Temperature-time curves of complete process of fire development. Theoretical study of wood fuel fires in enclosed spaces. *Acta Polytechnica Scandinavica* 1970; Ci 65, pp. 181 pp.-
- [2] Pettersson, Ove and Ödeen, Kai. *Brandteknisk dimensionering. Principer, underlag, exempel (In Swedish)*. LiberFörlag; Stockholm, Sweden. (1978)
- [3] König, Jürgen, Norén, Joakim, Olesen, Frits Bolonius, and Hansen, Finn Toft. Timber frame assemblies exposed to standard and parametric fires. Part 1 : Fire tests, *Report No. I 9702015*. SP Wood Technology: Borås, Sweden; Borås, Sweden. (1997)
- [4] *EN 1991-1-2, Eurocode 1: Actions on structures - Part 1-2: General actions - Actions on structures exposed to fire*. European Committee for Standardization; Brussels, Belgium. (2003)
- [5] Zehfuss, Jochen and Hosser, D. A parametric natural fire model for the structural fire design of multi-storey buildings. *Fire Safety Journal* 2007; **42**, Issue 115-126. 10.1016/j.firesaf.2006.08.004.
- [6] Zehfuss, Jochen. *Bemessung von tragsystemen mehrgeschossiger gebäude in stahlbauweise für realistische brandbeanspruchung*. Dr.-Ing., Carolo-Wilhelmina University of Technology at Brunswick, Lower Saxony, Germany; 2004)
- [7] Hakkarainen, Tuula. Post-Flashover fires in light and heavy timber construction compartments. *Journal of Fire Sciences* 2002; **20**, Issue March, pp. 133-175. [10.1177/0734904102020002074](https://doi.org/10.1177/0734904102020002074).

EXPERIMENTAL STUDY ON FIRE PROTECTION OF TIMBER ASSEMBLIES

Ni Zhaopeng^a, Qiu Peifang^b, Jim Mehaffey^c, Stan Winter^d

^a Senior Researcher of Code Division, Tianjin Fire Research Institute of China;

^b Assistant senior Researcher, Tianjin Fire Research Institute of China.

^c Scientist of Forintek Canada Corp., Canada;

^d Professor of Technical University of Munich, Germany.

INTRODUCTION

In the history of China, timber was once the main material for building dwellings. Even now, there are still lots of historic buildings built with heavy timbers. They have been standing there for hundreds of years.

Masonry, reinforced concrete and steel structures became the fashion of the last century. Therefore, fire protection researches were mostly focused on them, while timber fire protection was more or less neglected, especially during the last thirty years of 20th century. Accordingly, fire code of China at that time was focused on the requirements for masonry, concrete and steel structures too.

However, after China joined WTO, more and more wood councils and companies from North America, Europe and so on set up offices or branches in China to find market opportunities or promote cooperation with some research institutes and organizations with the purpose of studying the applicability and sustainability of wood frame buildings in China. As a result, a certain number of wood frame buildings (mostly single-family dwellings) have been built in Beijing, Tianjin, Shanghai, Hangzhou, Qingdao, Dalian, Guangzhou etc. In order to provide proper regulations for the construction and fire protection of wood frame buildings, a series of codes have been issued. For example, *Code for Quality Acceptance of Timber Structure Engineering* in 2002, *Code for Design of Timber Structures* in 2003, *Technical Code for Partitions with Timber Framework* in 2005 and *Code of Design on Building Fire Protection and Prevention* in 2006. However, the fire protection requirements in these codes need to be further improved and coordinated.

The requirements of current national fire code *Code of Design on Building Fire Protection and Prevention* (2006 edition) for timber fire protection are not specific enough. They can't meet the need of current China building construction market.

Therefore, Tianjin Fire Research Institute of MPS set up a joint technical committee with Canada Wood Council, European Wood Council and AF&PA from USA in September of 2005 to study the fire protection of timber structures. The cooperation has brought us great achievements and verification tests of timber elements were one of them. The data acquired from the tests can provide scientific support for the revision of current national fire code *Code of Design on Building Fire Protection and Prevention*.

The test assemblies were designed by European Wood council and constructed by Canada Wood council. The studs for wall assemblies, beams and columns were provided by European Wood Council, but all the other materials such as gypsumboard and rock fibre etc. were produced in China. These tests were done according to GB 9978 (equivalent to ISO 834) and observed by experts from Joint Technical Committee of China, Canada and Germany.

1. DESCRIPTION OF TEST ASSEMBLIES

Twelve full-scale timber building elements were tested in the lab of Tianjin Fire Research Institute.

They include 7 load-bearing or non-load-bearing exterior or interior wood stud walls, one independent ceiling, two floors, one gluelam beam and one gluelam column. Here only one wood stud wall test (load-bearing exterior wall) is introduced in detail. The furnace for conducting full-scale loaded/unloaded wall fire tests is shown in Figure 1. The opening of the wall furnace is 3m×3m. The details of the assemblies are given in Table 1.

Figure 1 Wall Furnace

Floor Furnace



Column Furnace



Table 1 Details of the tested assemblies

Time of testing	Name of the assembly	Fabrication	Dimension	Load	Result
Dec.19, 2007	Non-bearing exterior wall	gypsumboard -12mm; stud-89mm; glass wool -89mm; gypsumboard -12mm;	3270 × 3270 × 113		59min
Dec.20, 2007	Non-bearing exterior wall	Gypsumboard-15mm; stud-140mm; Rock fiber-140mm; gypsumboard -15mm;	3270 × 3270 × 170		99min
Jan.11,2008	Ceiling	gypsumboard-12mm; 30×50mm timber batten,	3500 × 4500		43min

		38×235 Truss rafter construction gypsumboard-12mm;	×289		
Jan.12,2008	Load-bearing exterior wall	Gypsumboard-15mm; wood stud-140mm, rock fibre-140mm; OSB-15mm OSB	3600 ×3300×170	22.5kN/m	64min
Jan.13,2008	Load-bearing interior wall	Gypsumboard-12mm; wood stud-89mm; glasswool-40mm; gypsumboard-12mm	3300 ×3600×113	11kN/m	47min
Jan.13,2008	Floor	Gypsumboard-12mm; Resilient metal slat-13mm; Beams-235mm Glass fibre>60mm; OSB-12mm	3065 ×4500 ×275	4kN/m	36min
Jan.16,2008	Load-bearing exterior wall	Gypsumboard-12mm; wood stud-89mm; glass fibre-80mm; OSB-12mm OSB	3600 ×3300×113	12.5kN/m	34min
Jan.17,2008	Load-bearing interior wall	Gypsumboard-15mm; Resilient metal slat-13mm; wood stud-89mm; rock fibre-80mm; Gypsumboard-15mm	3300 ×3600×132	2.5kN/m After reaching to 60min, increase 2.5kN every 5min.	72min
Jan.18,2008	Non-bearing interior wall	Gypsumboard-15mm; Wood stud-89mm; rock fibre-80mm; Gypsumboard-15mm;	3600 ×3300×243		183min
Jan.19,2008	Beam	Gluelam	200×400×5100	19kN/m	83min
Jan.20,2008	Floor	Two layers of gypsumboard-12mm Resilient metal slat-13mm Beam-235mm; rock fibre-80mm; OSB-18mm OSB	3065×4500 ×290	2.5kN/m	72min
Jan.23,2008	Column	Gluelam	200×280	Design load is 80kN , 4-face exposure	90min

2. DETAILS OF THE LOAD-BEARING EXTERIOR WOOD STUD WALL

2.1 Dimensions

The load-bearing wood stud wall assembly is 3600mm(wide)×3300mm(high)×170mm (thick).

2.2 Materials

The materials used in this wall assembly were gypsum boards, wood studs, rock fibre and OSB. Type H gypsum-board, conforming to the requirements of GB/T 9775 [EN 520 (Type F)] was used. The thickness of this kind of gypsum board was 15 mm. The framing materials of the wall assembly were wood studs (Solid Timber NH C24, conforms to EN 14081-1), 38 mm thick by 140 mm deep. The insulation for the assembly was rock fibre (density $\rho \geq 50 \text{ kg/m}^3$, melting point $>1000^\circ\text{C}$, which conformed to EN 13162 and GB/T 19686). OSB used in the unexposed surface of the wall assembly conformed to EN 300.

2.3 Fabrication

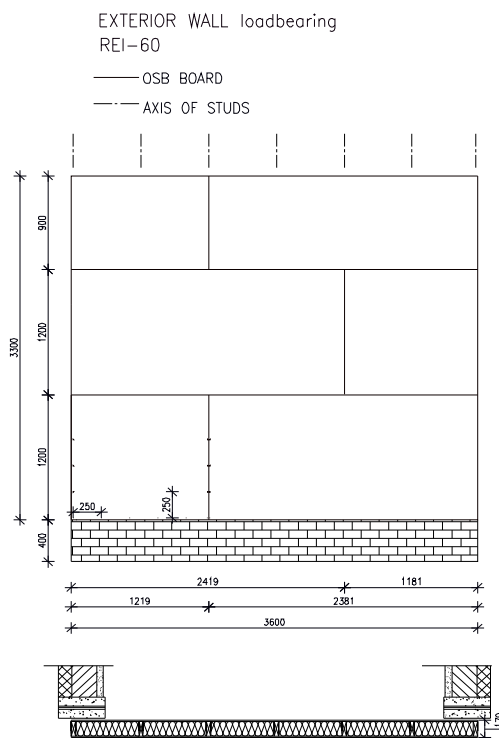
Fabrication details on the assembly is presented in Table 2.

Table 2 Fabrication of load-bearing exterior wall

No.	Component	Specification according to	Thickness [mm]	Cross section
1	Gypsum plasterboard Fastening: dry wall screw 3,5x50 all 250mm	EN 520 (Type F) GB/T 9775 (Type H)	15,0	
2	Studs b/h = 38/140 mm ² , e = 600 mm Fastening: (nails 3,8x75)	Solid Timber NH C24 EN 14081-1	140,0	
3	Mineral fibre insulation (rock fibre) density ≥ 50 kg/m ³ Melting point >1000°C	EN 13162 GB/T 19686	140,0	
4	OSB Fastening: (nails 3,3x65) all 250mm	EN 300 EN 13986	15,0	

All the test assemblies were constructed in the processing workshop of the lab. In this wall assembly, one layer of 15mm thick Type H gypsum board was attached vertically to the wood studs on the exposed side with drywall screws, 50mm long, and spaced at 250 mm O.C. along the edges and in the field of the board. Screw locations and gypsum board joints are shown in Figure 2. The screw heads on both the exposed and unexposed faces were covered with joint compound. The gypsum board joints were finished with fibre tape and covered with joint compound.

Figure 2 Screw locations and gypsum board joints



3. TEST CONDITIONS AND PROCEDURES

3.1 Instrumentation

Type K (20 gauge) chromel-alumel thermocouples were used for measuring temperatures at a number of locations throughout an assembly.

Thermocouple locations on the unexposed surface of the wall assembly are shown in Figure 3.

Figure 3 Locations of thermocouples

Figure 4 Loading device



3.2 Loading System

The loading device used in this study is illustrated in Figure 4. The components of this device are a strong steel frame, in which the wall assembly is placed, and 9 hydraulic jacks fitted at the top to simulate vertical structural loads. The applied loading on the wall assembly used in this assembly was 22.5Kn/m.

3.3 Test Procedure

The test was carried out by exposing the assemblies to heat in a diesel-fired vertical furnace as shown in Figure 1. The assembly was sealed at the edges against the furnace using ceramic fibre blankets. The furnace temperature was measured by 7 shielded thermocouples in accordance with GB/T 9978. The average of the 7 thermocouple temperatures was used to control the furnace temperature.

3.4 Fire Exposure

During the test, the wall assembly was exposed to heating on the exposed side, in such a way that the average temperature in the furnace followed, as closely as possible, the GB/T 9978 [10] (equivalent to ISO 834) standard time-temperature curve.

3.5 Failure Criteria

The failure criteria were derived from GB/T 9978 [10]. The assembly was considered to have failed if a single point thermocouple temperature reading on the unexposed face rose 180°C above ambient or the average temperature of the 9 thermocouple readings under the insulated pads on the unexposed face (see Figure 3) rose 140°C above the ambient temperature or there was passage of flame or gases hot enough to ignite cotton waste. The test assembly was also deemed to have

structurally failed if there was excessive (>150 mm) deflection.

3.6 Recording of Results

The furnace and wall assembly temperatures were recorded at 1 minute intervals through computer data acquisition system. The gauge pressure of the loading system was also recorded at 1 minute intervals.

3.7 Observations

Observation during fire test 12th of January 2008, exterior wall REI-60

time [min:s]	Observation during fire test	Side of observation
0:00	start (manual burner start)	-
2:00	black coloring of paper lamination fire exposed gypsum board	E
7:30	surface of gypsum boards becomes white again, cracks in puddy	E
22:00	puddy in joints fall down	E
25:00	flammable gases escapes from joints inside the furnace	E
32:00	visible burning of studs under joints	E
45:00	escape of Smoke at horizontal OSB joint	UE
55:00	Increase of smoke	UE
64:00	stop of testing, (break off by test institute) large horizontal deflection, escape of flames between furnace and assembly no integrity failure of assembly only brown colouring at OSB joint	UE

*) F – fire exposed side; UE – fire unexposed side

4. TEST RESULTS

For this exterior wall assembly, the design time was REI 60min. The ultimate result was 64min, which was within our expectation. It failed structurally through excessive deflection. The unexposed surface temperature at the time of structural failure was below the temperature failure criteria.

5. CONCLUSIONS

With the help of these verification tests, we have obtained the fire resistance ratings of some typical wood stud walls, floor and gluelam beams and columns as well as their burning behaviors under standard fire. The data obtained from these tests agree well with those obtained from the similar assembly tests done in Canada and Germany. It indicates that China building and fire code can adopt the data of those timber assemblies listed in the building codes of those countries like Canada. Of course, we will do further research on timber fire protection so as to provide more scientific supports for the revision of China building and fire code.

6. REFERENCE

1. GB/T 9978-2008: Fire-resistance tests-Elements of building construction-Part 1: General requirements (ISO 834-1: 1999, MOD).
2. NO.2008-0217: Testing Report. National Center for Quality Supervision and Test of Fixed Fire-fighting Systems and Fire-resisting Building Components of China, 2008.

FIRE RESISTANCE OF TRUSSES WITH PUNCHED METAL PLATE FASTENERS

Petr Kuklík^a, Jan Starý^b, Aleš Tajbr^a, Miloš Vodolan^b

^a Czech Technical University in Prague, Faculty of Civil Engineering, Prague, Czech Republic

^b FINE s.r.o., Prague, Czech republic

INTRODUCTION

Great attention in the Czech Republic is paid to development of software and methodology of analysis of timber structures with punched metal plate fasteners. Company FINE s.r.o. in cooperation with the fastener producer BOVA Březnice and CTU in Prague, Faculty of Civil Engineering, has been developing program TRUSS for analysis and design of these structures using the modern technology. At the same time, a research of behaviour of punched metal plate fasteners at normal temperature and in fire has been carried out.

1 DESCRIPTION OF FIRE TESTS

Geometry and load layout of tested structures were designed to represent common conditions of real structures. The aim of the first experiment was to find the real fire resistance of timber structures connected by punched metal plate fasteners. The second test was performed to determine the influence of simple construction arrangements on increase of fire resistance of the same structure.

1.1 Fire test No. 1

The structure consisted of three flat trusses – see *Fig. 1*. The thickness of timber members was 50 mm, the truss span was 6,0 m and the truss spacing was 1,0 m. The trusses were made of timber of grade S10 (C24) and punched metal plate fasteners BV15 and BV20 were used. The structure was diagonally braced by 120x24 mm members installed in planes of all verticals and upper chords. The top chord was sheathed with 120x24 mm boards and there was no ceiling. The load was determined according to EN 1990 and the trusses were designed in program TRUSS 4. The temperature during the fire test corresponded to the time-temperature curve according to EN 1995-1-2. *Fig. 2* and *Fig 3* show the tested structure.

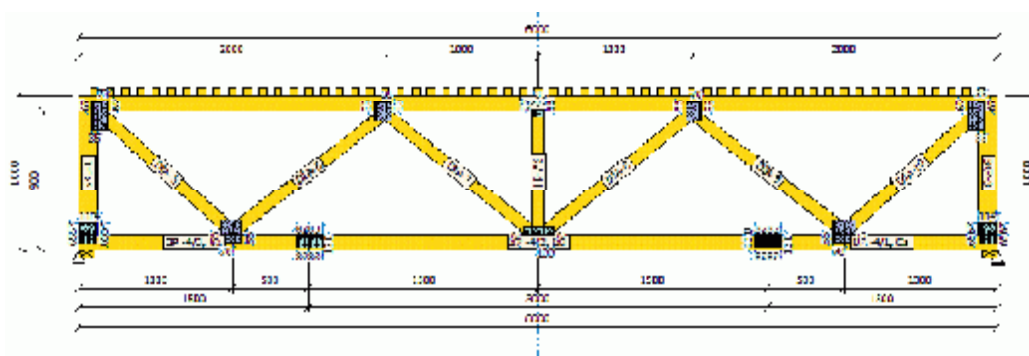


Fig.1. Drawing of the truss used for the fire test



Fig.2. Structure No. 1 before the fire test



Fig.3. Structure No.1 during the fire test

The test results demonstrated that fire resistance of timber structures with punched metal plate fasteners is not insignificant. The second limit state (deflection and rate of deflection increase) was reached after 8 minutes. The structure collapsed (reached the first limit state) in the 11th minute of the test. These results were quite encouraging therefore it was decided to perform a second test on the same structure but with some arrangements to increase its fire resistance.

1.2 Fire test No. 2

The first fire test indicated that the decisive elements for fire resistance of the structure are the punched metal plate fasteners located in splice of lower chords of trusses. They are the most fire-exposed elements in the structure and their failure quickly leads to collapse of the structure. So it is expected that if this critical point is improved, the fire resistance could increase. Therefore fire test No. 2 was performed. The second structure was the same as the first one except that the punched metal plate fasteners in splice of lower chords of trusses were overlapped with timber elements as shown in *Fig. 4*.

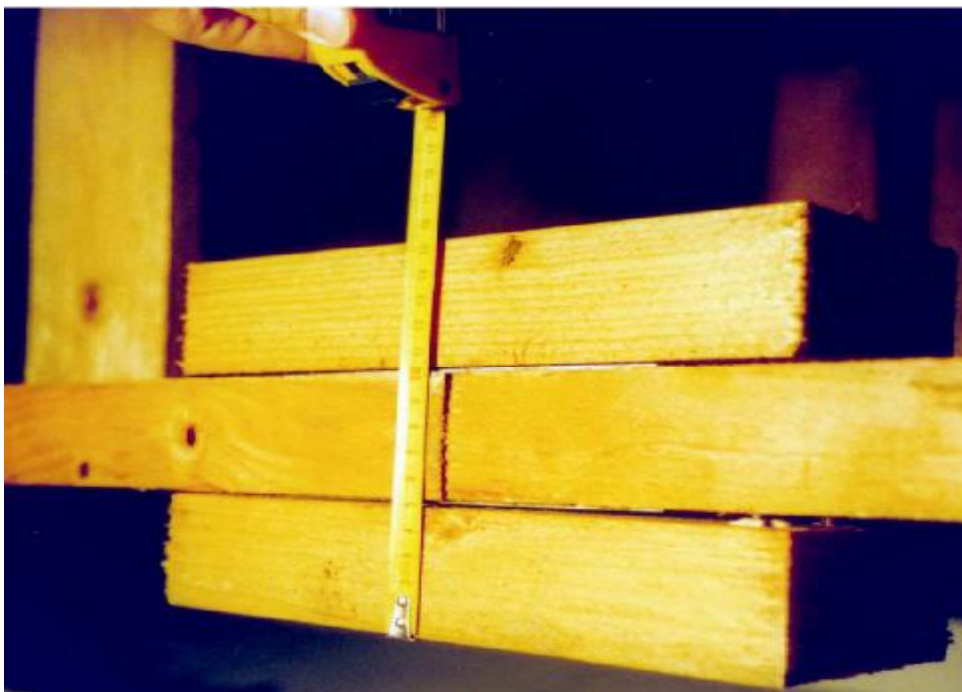


Fig.4. Detail view of overlap of a lower chord splice

Test No. 2 was performed at the same conditions as the test No. 1 and the results were positive. The second limit state was reached after 11 minutes and it means the 35% increase of fire resistance with respect to the test No. 1.

2 SUMMARY AND ACKNOWLEDGMENT

Two fire tests, performed in the Fire laboratory of PAVUS in Veselí nad Lužnicí, proved that structures with punched metal plate fasteners by themselves have some fire resistance, which is not insignificant and could be taken into account in structure fire-design. Fire test No. 2 showed that the overlap of splice joint of lower chords with timber elements is a simple and cheap modification, which positively affects fire resistance of these structures.

It is expected to perform sufficient number of similar tests required for significant statistical evaluation. However the two tests are useful pieces in the puzzle of knowledge of fire behaviour of these structures.

The anchorage strengths (5-percentile values) of punched metal plate fasteners BV15 and BV20 produced by BOVA Březnice and determined from tests at normal temperature according to EN 1995-1-1 and EN 14545 are showed in *Fig. 5*.

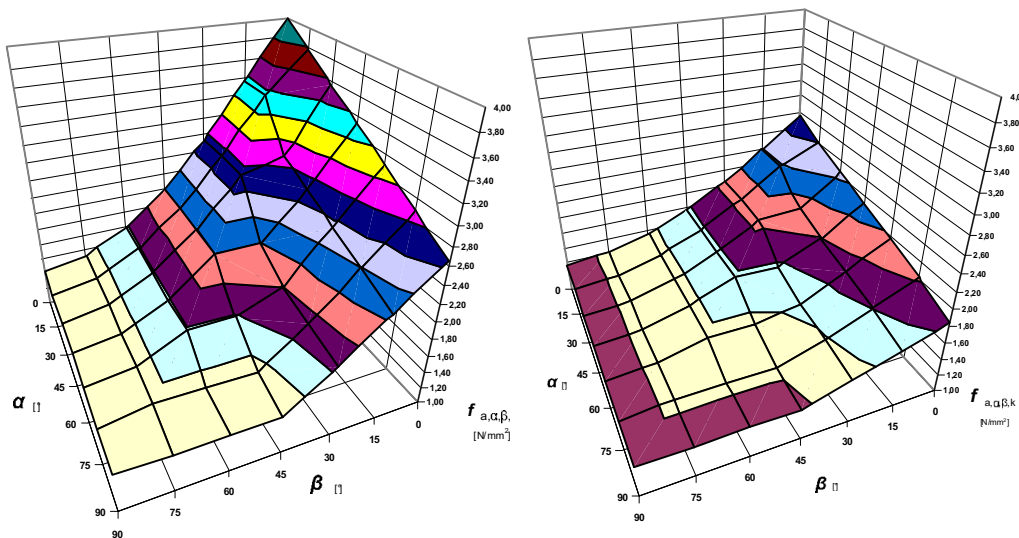


Fig.5. Anchorage strengths of punched metal plate fasteners BV15 and BV20

The article was created under the support of the research aim of CTU in Prague MSM 6840770005 "Sustainable Construction".

REFERENCES

- [1] EN 1990 Eurocode: Basis of structural design
- [2] EN 1995-1-1 Eurocode 5: Design of timber structures - Part 1-1: General rules and rules for buildings
- [3] EN 1995-1-2 Eurocode 5: Design of timber structures - Part 1-2: Structural fire design
- [4] EN 14545 Timber structures - Connectors - Requirements